

## Multiband theory of quantum-dot quantum wells: Dim excitons, bright excitons, and charge separation in heteronanostructures

W. Jaskólski\* and Garnett W. Bryant†

National Institute of Standards and Technology, Gaithersburg, Maryland 20899

(Received 5 September 1997; revised manuscript received 24 November 1997)

Electron, hole, and exciton states of multishell CdS/HgS/CdS quantum-dot quantum-well nanocrystals are determined by use of a multiband theory that includes valence-band mixing, modeled with a six-band Luttinger-Kohn Hamiltonian, and nonparabolicity of the conduction band. The multiband theory correctly describes the recently observed dim-exciton ground state and the lowest, optically active, bright-exciton states. Charge separation in pair states is identified. Previous single-band theories could not describe these states or account for charge separation. [S0163-1829(98)52108-X]

Quantum-dot quantum-well (QDQW) nanocrystals are composed of an internal semiconductor core that is coated with several shells of different semiconductors.<sup>1,2</sup> These structures have been synthesized by wet chemistry and can have spherical<sup>3</sup> or tetrahedral<sup>1</sup> shape. The method of covering CdS or HgS nanocrystals by HgS or CdS shells has been established for several years.<sup>4</sup> Recently, QDQW's containing three layers, each with a thickness controlled to a single monolayer,<sup>3,5</sup> have been fabricated. Transition energies and optical dynamics in these structures can be precisely designed by changing the internal core diameter and thickness of each shell. With the possibility of achieving very uniform size distributions of dots in a sample and the ability of forming two-dimensional (2D) and three-dimensional (3D) arrays of chemically synthesized nanocrystals,<sup>6</sup> QDQW's become intriguing candidates as building blocks in QD arrays for novel electronic and optical applications.

Recently, Mews *et al.*<sup>1</sup> fabricated and studied QDQW nanocrystals formed with 4–5-nm-diam CdS cores, 1-ML HgS shells, and ~2-nm-wide CdS outer cladding layers. Since CdS has a wide band gap and HgS has a narrow band gap, the radial profiles for conduction-band (CB) and valence-band (VB) edges of a CdS/HgS/CdS QDQW each form an internal quantum well in the HgS layer. The electron-hole excitations in these structures are determined by competition between global confinement in the entire nanocrystal, local confinement in the internal quantum well, and electron-hole pair interaction.

The low-energy optical excitations in these QDQW's have been measured by absorption, luminescence, fluorescence line narrowing (FLN), and hole burning (HB).<sup>1</sup> The lowest optically active electron-hole pair state is separated from the next optically active pair state by about 60 meV. A large, 19-meV Stokes energy shift is observed between the lowest optically active pair state, which is used as the excitation level in the fluorescence measurements, and the main emission peak. This Stokes shift indicates that the ground state is a *dim* exciton that is only weakly optically active, but does not determine whether the dim exciton is a dark exciton, optically forbidden due to exchange effects, or a spatially indirect exciton.

Electron, hole, and exciton states of QDQW's have been investigated so far only with the one-band effective-mass

approximation, treating a light hole with a mass similar to the CB mass.<sup>2,3,7</sup> The energy of the main absorption peak can be predicted reasonably well by these calculations. However, in these calculations, the main absorption peak arises from transitions to the lowest pair state, and there is no dim-exciton ground state. Also, the next optically active pair state is predicted to be 200 meV above the lowest optically active state. Since the electron and hole have similar masses in these models, little separation of the electron and hole into different layers is predicted.

The presence of multiple, closely spaced excitations with very different oscillator strengths suggests that a more detailed description of the band states, including both heavy and light holes, is needed for these QDQW's. It has been proved for other semiconductor quantum dots<sup>8–11</sup> that valence-band mixing must be included to correctly describe hole levels, transition energies, and excitation spectra. For structures containing layers of narrow-gap semiconductors, such as HgS, CB nonparabolicity should also be included. To explain the recently observed spectra of CdS/HgS/CdS quantum dots,<sup>1</sup> to determine when charge separation occurs, and to study how energy levels and excitation spectra depend on CdS and HgS shell thicknesses, we have performed multiband calculations for spherical QDQW's based on the  $\mathbf{k} \cdot \mathbf{p}$  method and the envelope function approximation (EFA).

We use the six-band Luttinger-Kohn Hamiltonian in the spherical approximation<sup>8,12</sup> to describe holes. Only the angular momentum  $F=J+L$  [where  $J$  is the Bloch band-edge angular momentum ( $\frac{3}{2}$  for heavy and light holes and  $\frac{1}{2}$  for split-off holes) and  $L$  is the envelope angular momentum in a spherical dot] commutes with the hole Hamiltonian. The hole states are eigenfunctions of  $F$  and  $F_z$ ,

$$|FF_z; nL^h\rangle = \sum_{J,L \geq \frac{1}{2}} \sum_{J_z, L_z} \langle JJ_z LL_z; FF_z | JJ_z \rangle |nLL_z\rangle, \quad (1)$$

where  $|JJ_z\rangle$  are the appropriate Bloch band-edge states,  $\langle \mathbf{r} | nLL_z \rangle = f_{nL}(r) Y_{LL_z}(\hat{\mathbf{r}})$ ,  $f_{nL}(r)$  are radial envelope functions, and  $Y_{LL_z}(\hat{\mathbf{r}})$  are spherical harmonics. Following Ref. 9, hole states are described by the notation  $nL_F^h$  that indicates the hole radial quantum number  $n$ , the hole total

angular momentum  $F$ , and  $L^h$ , the lowest  $L$  that appears in Eq. (1) for a given  $F$ . The three different radial components  $f_{nL}(r)$  that appear for a given  $F$  are solutions of a set of second-order coupled differential equations for the radial part of the six-band Luttinger-Kohn Hamiltonian. For each semiconductor shell this Hamiltonian depends on three empirical parameters: two Luttinger parameters  $\gamma$  and  $\gamma_1$  and the split-off gap  $\Delta$ .

The electron states are products of the Bloch CB edge state  $|S\sigma\rangle$  for an  $S$  atomic state with spin  $\sigma$  and the envelope functions  $|nL^eL_z^e\rangle$ . The one-band effective-mass radial equation is solved numerically to determine  $f_{nL^e}(r)$ . CB nonparabolicity is included perturbatively in the radial equation by use of an energy-dependent mass correction defined by the energy gap  $E_g$  and  $E_p = 2V^2$ , where  $V = \langle S|p_z|Z\rangle$  is the Kane matrix element.<sup>9</sup>

We use the following parameters: CdS  $E_g = 2.5$  eV,  $\gamma_1 = 0.814$ ,  $\gamma = 0.307$ ,  $\Delta = 0.08$  eV,  $E_p = 19.6$  eV; HgS  $E_g = 0.2$  eV,  $\gamma_1 = 12.2$ ,  $\gamma = 4.5$ ,  $\Delta = 0.08$  eV,  $E_p = 21.0$  eV. Heavy- and light-hole (hh and lh) masses resulting from  $\gamma$ ,  $\gamma_1$  are CdS  $m_{hh} = 5.0$ ,  $m_{lh} = 0.7$ ; HgS  $m_{hh} = 0.31$ ,  $m_{lh} = 0.047$ . These parameters are close to literature values.<sup>13–17</sup> The HgS band gap is taken to be positive, consistent with recent photoemission measurements of the HgSe gap.<sup>18</sup> Previous experiments suggest an inverted HgS band structure with a negative gap.<sup>15</sup> Most states that we study lie away from the HgS band gap, due to high confinement energy in the narrow HgS shell, and should not depend strongly on the exact value of the HgS gap. Based on CdS and HgS photoelectric thresholds,<sup>19</sup> CB and VB offsets are taken to be 1.45 and 0.85 eV, respectively, close to values in previous calculations.<sup>2,3,7</sup> Electron and hole barriers for tunneling into water, which is the medium surrounding the QDQW, are 4 eV (H<sub>2</sub>O photoelectric threshold is  $\approx 8$  eV) when measured from the HgS midgap. H<sub>2</sub>O masses are  $m_{hh} = m_{lh} = m_e = 1.0$  ( $\gamma_1 = 1.0$  and  $\gamma = 0.0$ ).<sup>7</sup> The choice of H<sub>2</sub>O masses is not critical since high H<sub>2</sub>O barriers prevent significant leakage from the QDQW. Contribution from higher electron bands is included by use of the parameter  $f = -1.0$  in the electron effective-mass equation.<sup>9</sup> The resulting electron mass is 0.15 near the CdS CB edge and 0.04 for the energy range of interest in HgS, close to literature values.<sup>7,14,15</sup>

We perform multiband calculations to study QDQW's because full electronic structure calculations are difficult. However, it is not clear that the EFA and the effective-mass approximation can be applied to QDQW's with layers as thin as 1 ML and energy levels far from band edges. We test the usefulness of applying the EFA to thin-layer QDQW's by performing calculations for wide-layer structures, where the EFA works well,<sup>9–11</sup> and then reducing shell widths to reach the thin-layer limit. The sequence of calculations is shown in Fig. 1. We start with a 2-nm-radius CdS dot, i.e., a 1-nm core and a 1-nm clad [structure (a) in Fig. 1]. Next, we add a HgS shell between the core and clad, starting with a 0.3-nm ( $\sim 1$ -ML) shell and extending to a 2-nm shell [structure (b) in Fig. 1]. Next the CdS core is reduced until the limit of a HgS/CdS dot with no core [structure (c)] is reached. Finally, the 1-nm-wide CdS clad is eliminated to end with a 4-nm-diam HgS QD [structure (d)].

Electron and hole energies are shown in Fig. 2 for this sequence of structures. Transition energies  $E_{tr}$  are calculated

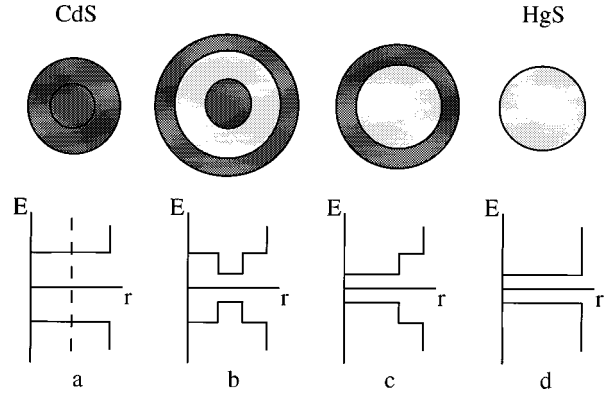


FIG. 1. The sequence of CdS/HgS/CdS quantum-dot quantum wells investigated and the corresponding schematic layout of CB and VB edges.

by taking the electron-hole pair energy differences and subtracting the pair binding energy, which is determined perturbatively<sup>20</sup> with an average effective dielectric constant. The rates for these transitions are proportional to

$$(1/E_{tr}) \sum_{L_z^e \sigma} \sum_i |\sum_{F_z J_z} \langle JJ_z LL_z; FF_z \rangle \langle n^e L^e L_z^e | n^h LL_z \rangle| \times \langle S\sigma | \hat{p}_i | JJ_z \rangle|^2. \quad (2)$$

The rates are averaged over the final electron state and the linear polarization ( $i$ ) of the dipole transition operator, which is proportional to the momentum  $\hat{p}$ . Energies and relative

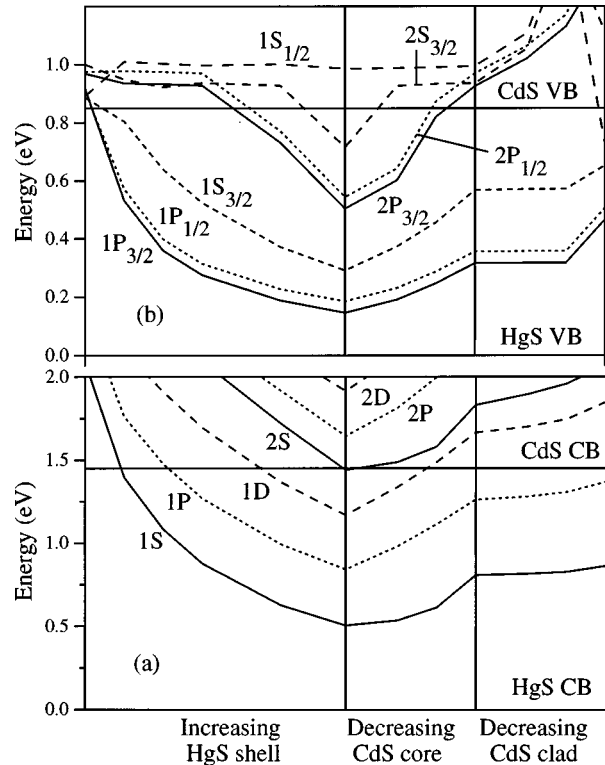


FIG. 2. The lowest electron (a) and hole (b) energy levels for the sequence of structures shown in Fig. 1. Left part: HgS shell increases from 0 to 2 nm (from left to right); middle: CdS core decreases from 1 to 0 nm; right: CdS clad decreases from 1 to 0 nm.

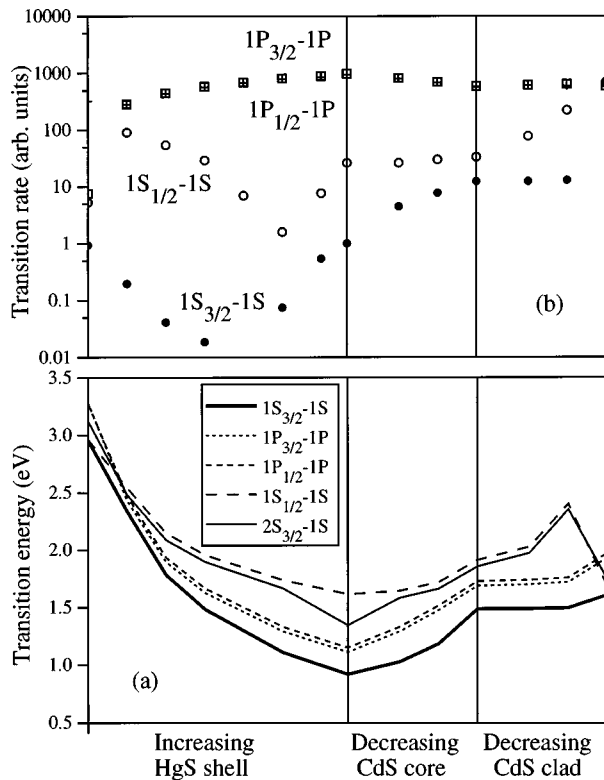


FIG. 3. Transition energies (a) and relative transition rates (b) for the QDQW sequence in Fig. 1.

rates for the lowest transitions are shown in Figs. 3(a) and 3(b). Electron and hole levels evolve smoothly as layer thicknesses are varied. The EFA, which accurately describes wide-layer structures, should still provide reasonable results for thin-layer QDQW's.

As the HgS shell width increases, successive electron states become trapped in the HgS shell when their energies fall below the CdS CB edge and their charge densities become localized in the HgS shell. Due to global confinement, electron energies increase as the CdS core or clad decreases. In the one-band approximation,<sup>2,3,7</sup> hole and electron states behave the same way when the HgS thickness is varied, with the corresponding hole and electron states trapping in the HgS for nearly the same thickness. In the multiband approximation, hole states behave differently from electron states. A group of hole levels ( $1P_{3/2}$ ,  $1P_{1/2}$ ,  $1S_{3/2}$ ) easily fall below the CdS VB edge, even for a HgS shell as thin as 1 ML ( $\sim 0.3$  nm). The corresponding charge densities are strongly localized inside the HgS (see Fig. 4). These hole states are more easily trapped than the corresponding electron states. The  $n=2$  hole states of these symmetries trap in the HgS layer at larger widths ( $\sim 0.4$ – $0.5$  nm). There is also a group of states ( $nS_{1/2}$ ) with energies above the CdS VB edge even for a 2-nm-wide HgS shell. Their charge density maxima are located in the CdS cladding layer (see Fig. 4).

The  $1S_{1/2}$  hole state does not trap in the HgS layer because the CdS and HgS hole effective masses are so different. The  $1S_{1/2}$  state is made from light-hole and split-off bands only. The HgS light-hole and split-off band masses are about 15 times lighter than the corresponding CdS masses. The HgS shell cannot confine the  $S_{1/2}$  state, even though the HgS shell is a potential well, because the hole has such a

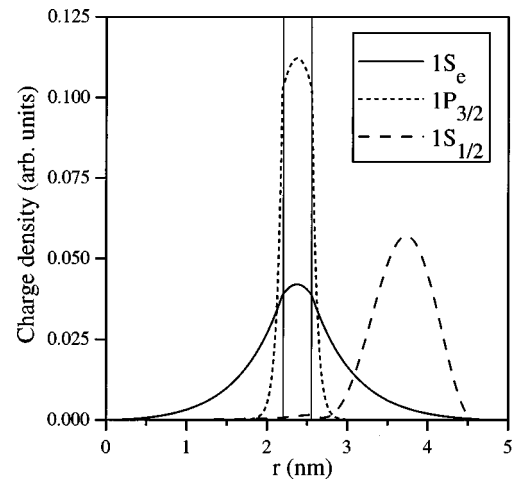


FIG. 4. Charge densities of several electron and hole states for a CdS/HgS/CdS QDQW with CdS core, radius 2.2 nm, 0.35 nm HgS shell, and 2 nm CdS clad. Vertical bars mark the HgS shell.

light mass and high kinetic energy in that shell. Moreover, the dominant contribution from the  $J=\frac{3}{2}$  band to the lowest  $S_{1/2}$  state is made by the  $L=2$  component.<sup>8,10</sup> Thus the  $S_{1/2}$  charge-density maximum is in the CdS clad. In contrast,  $S_{3/2}$ ,  $P_{3/2}$ , and  $P_{1/2}$  states are a mixture of heavy-hole, light-hole, and split-off bands. The HgS heavy-hole mass and the CdS light-hole mass are similar, so these states can localize in the HgS well.

Localization of the hole  $1S_{1/2}$  state in the CdS clad and the electron  $1S$  state in the HgS shell (see Fig. 4) explains why the rate [Fig. 3(b)] of the  $1S_{1/2}-1S$  transition is about two orders of magnitude smaller than those of the  $1P_{3/2}-1P$  or  $1P_{1/2}-1P$  transitions. Including the effects of pair interaction beyond the perturbation energy shift included in our calculations would not dramatically reduce this charge separation because quantum confinement effects dominate pair binding in these small structures.<sup>7</sup> The binding energy of an exciton in this pair state should be smaller than in other pair states, because the electron and hole are localized in different layers. The rate for the  $1S_{3/2}-1S$  transition is even smaller than for the  $1S_{1/2}-1S$  transition. Only the  $L=0$  component of the  $1S_{3/2}$  state has a nonvanishing transition dipole. In these QDQW structures this component of the hole state is negligible compared to the two  $L=2$  components, so the  $1S_{3/2}-1S$  transition is optically inactive.

Finally, we perform specific calculations for the QDQW's investigated by Mews *et al.*<sup>1</sup> We consider a QDQW with a 2.2-nm-radius CdS core, 1-ML (0.35 nm) HgS shell and 2-nm-wide CdS clad. The calculated energies of the first two optically active transitions,  $1P_{3/2}-1P$  and  $1P_{1/2}-1P$ , are 1.890 and 1.929 eV, respectively. In the HB experiment by Mews *et al.*<sup>1</sup> and Banin and Mews,<sup>21</sup> the first excitation peak appears at 1.878 eV, only 12 meV different from the calculated energy of the lowest  $1P_{3/2}-1P$  electron-hole pair state. The next experimentally observed excitation is  $\sim 60$  meV higher (Fig. 2 of Ref. 1) and differs from the predicted position of the  $1P_{1/2}-1P$  state by only 10 meV. Experimentally, both transitions should be of comparable strength.<sup>21</sup> Our calculated transition rates are almost the same for these transitions [see Fig. 3(b)]. The calculated energy of the optically weak  $1S_{3/2}-1S$  transition is redshifted from the

ground  $1P_{3/2}-1P$  transition by 18 meV, almost exactly the 19-meV shift observed between absorption and emission peaks in FLN (Fig. 2 of Ref. 1). Thus the  $1S_{3/2}-1S$  state is the *dim exciton* in this structure. The energy shift  $\Delta_{\text{HB-FLN}}$  between the *excitation* peaks of HB and FLN spectra shown in Fig. 2 of Ref. 1 most likely occurs because the samples contain a distribution of QDQW's. The lowest calculated transition redshifts approximately by  $\Delta_{\text{HB-FLN}}$  when the CdS core radius increases to 2.8 nm.

In conclusion, a multiband theory of electron, hole, and exciton states in QDQW's has been developed. Multiband calculations show that for some pair states, the electron and hole can be trapped in different shells, yielding weak oscillator strengths for these transitions. Other transitions can be

weak even if both electron and hole are localized in the same layer. The observed energy difference between the lowest optically active transitions in CdS/HgS/CdS QDQW's and the appearance of a *dim-exciton* ground state can be explained by the multiband-theory. This could not be done in the one-band approximation. These results show that the EFA can be used to interpret optical spectra of QDQW's containing layers as thin as 1 ML. For a more accurate description, corrections beyond the EFA, due to any nonspherical shape of the dots, pair exchange, and correlation should also be included.

Support from The Fulbright Foundation and KBN Project No. 2 PO3B 156 10 is gratefully acknowledged.

\*Permanent address: Instytut Fizyki UMK, Toruń, Poland.

<sup>†</sup>Electronic address: garnett.bryant@nist.gov

<sup>1</sup>A. Mews, A. V. Kadavanich, U. Banin, and A. P. Alivisatos, *Phys. Rev. B* **53**, R13 242 (1996).

<sup>2</sup>D. Schooss, A. Mews, A. Eychmüller, and H. Weller, *Phys. Rev. B* **49**, 17 072 (1994).

<sup>3</sup>A. Mews, A. Eychmüller, M. Giersig, D. Schooss, and H. Weller, *J. Phys. Chem.* **98**, 934 (1994).

<sup>4</sup>A. Eychmüller, A. Hässelbarth, and H. Weller, *J. Lumin.* **53**, 113 (1992).

<sup>5</sup>A. Hässelbarth, A. Eychmüller, R. Eichberger, M. Giersig, A. Mews, and H. Weller, *J. Phys. Chem.* **97**, 5333 (1993).

<sup>6</sup>C. R. Kagan, C. B. Murray, M. Nirmal, and M. G. Bawendi, *Phys. Rev. Lett.* **76**, 1517 (1996).

<sup>7</sup>G. W. Bryant, *Phys. Rev. B* **52**, R16 997 (1995).

<sup>8</sup>G. B. Grigoryan, E. M. Kazaryan, A. L. Efros, and T. V. Yazeva, *Sov. Phys. Solid State* **32**, 1031 (1990).

<sup>9</sup>A. I. Ekimov *et al.*, *J. Opt. Soc. Am. B* **10**, 100 (1993).

<sup>10</sup>D. J. Norris and M. G. Bawendi, *Phys. Rev. B* **53**, 16 338 (1996).

<sup>11</sup>W. Jaskólski and G. W. Bryant (unpublished).

<sup>12</sup>A. Baldereschi and N. O. Lipari, *Phys. Rev. B* **8**, 2697 (1973).

<sup>13</sup>C. Herman and C. Weisbuch, in *Optical Orientation*, edited by F. Meyer and B. P. Zakharchenya (Elsevier, Amsterdam, 1984).

<sup>14</sup>B. F. Bielin'kii, R. V. Garasimchuk, M. V. Kurik, and M. V. Pashovskii, *Sov. Phys. J.* **12**, 973 (1969).

<sup>15</sup>I. Broser, R. Broser, and M. Rosenzweig, in *Numerical Data and Functional Relationships in Science and Technology*, edited by O. Madelung, Landolt-Börnstein, New Series, Group III, Vol. 17, Pt. 3.10 (Springer-Verlag, Berlin, 1982), G. Nimitz in *ibid.*, Pt. 314.

<sup>16</sup>G. L. Bir and G. E. Pikus, in *Symmetry and Strain-Induced Effects in Semiconductors*, Israel Program for Scientific Translations, Jerusalem (Wiley, New York, 1975).

<sup>17</sup>Not all of these parameters are well known, particularly for HgS. Our choices are best estimates from the available values.

<sup>18</sup>K.-U. Gawlik *et al.*, *Phys. Rev. Lett.* **78**, 3165 (1997).

<sup>19</sup>A. H. Nethercot, *Phys. Rev. Lett.* **33**, 1088 (1974).

<sup>20</sup>L. E. Brus, *J. Chem. Phys.* **80**, 4403 (1984).

<sup>21</sup>U. Banin and A. Mews (private communication).